International Journal of Current Advanced Research
ISSN: O: 2319-6475, ISSN: P: 2319-6505, Impact Factor: 6.614
Available Online at www.journalijcar.org
Volume 10; Issue 02 (A); February 2021; Page No.23741-23745
DOI: http://dx.doi.org/10.24327/ijcar.2021.23745.4707

Research Article

THE SIMILAR CHARACTERISTICS OF VARIOUS ILLNESS

Guliko Kiliptari[1]., Grigol Nemsadze[2] and Miranda Kokhreidze[3]

[1]Critical Care Department of University Clinic after Acad. Kipshidze, Prof. of TSMU (Tbilisi, Georgia)
[2]Radiology Department of University Clinic after Acad. Kipshidze, Prof. of TSMU (Tbilisi, Georgia)
[3]Doctor of University Clinic after Acad. Kipshidze, (Tbilisi, Georgia)

A R T I C L E I N F O

Article History:
Received 6th November, 2020
Received in revised form 15th December, 2020
Accepted 12th January, 2021
Published online 28th February, 2021

Key words:
Covid-19, HIV, Respiratory distress-syndrom

A B S T R A C T

COVID-19 pneumonia manifests with chest CT imaging abnormalities, bilateral, subpleural, ground-glass opacities with air bronchograms. Different radiological patterns are observed at different times throughout the disease course. Diffuse bilateral ground-glass opacities co-existes or progresses with consolidations and fibrosis. Evaluation of imaging features, clinical and laboratory findings could to diagnosis of COVID-19 pneumonia and assessment of prognostic values.

We presented cases to analyse the chest CT imaging features in patients with COVID-19 pneumonia, to compare the imaging and laboratory data to across the disease course and to other severe infection, like pneumocyst pneumonia.

Conclusion: Evaluation of blood tests and comparison of clinical data made it possible to diagnose a similare in the course of and CT findings, but of absolutely different disease. This comparison allow distinguish similar characteristics of different diseases and make prognostic conclusions during the course and treatment of illness**.**

INTRODUCTION

COVID-19 pneumonia manifests with chest CT imaging abnormalities, bilateral, subpleural, ground-glass opacities with air bronchograms. Different radiological patterns are observed at different times throughout the disease course. Diffuse bilateral ground-glass opacities co-existes or progresses with consolidations and fibrosis. Evaluation of imaging features, clinical and laboratory findings could to diagnosis of COVID-19 pneumonia and assessment of prognostic values.

We presented cases to analyse the chest CT imaging features in patients with COVID-19 pneumonia, to compare the imaging and laboratory data to across the disease course and to other severe infection, like pneumocyst pneumonia. This comparison allow distinguish similar characteristics of different diseases and make prognostic conclusions during the course and treatment**.**

Case presentation

Patient 1

A 50 old man was admitted to aour hospital with one week history of fever, dry cough, he reported to reduced appetite and altrered sens of taste. Chest radiography displays -Breast contour without deformation. Lymphadenopathy is not expressed.

Corresponding author:* **Guliko Kiliptari
Critical Care Department of University Clinic after Acad. Kipshidze, Prof. of TSMU (Tbilisi, Georgia)

The main bronchi recede. The size of the heart is not enlarged. The amount of fluid in the pericardial cavity is not increased.

Infiltrative changes in bilateral lung parenchyma are reflected in subtotal infiltrative changes of the ground glass type, the density of which is higher in the lower extremities, where areas of consolidation and thicker areas in adults are revealed. Relatively small volume consolidations are also reflected in the upper rates. The intervertebral pleura is thickened. In the bilateral pleural cavity, a small amount of separated, free air was not found. Semi-quantitative methodological analysis of computed tomography data, index of lung damage - 21 points (0-24). Angiographic examination showed no filling defect of the pulmonary trunk and bilateral main, parietal arteries.

Aggravation of respiratory parameters despite NIV and HFNC, has lead to mechanical ventilation. Severe respiratory distress syndrom was treated with suitable strategy of ventilation and patient state was managed with foreseeing of all clinical and laboratory parameters Laboratory studies showed increased level of leuvocytes, CRP, IL_6, Liver enzymes.

Humoral immunity and cell-mediated immunity

Table 1

CD3 %/ 10^9 /l	62	59	IgG g/l	11	13.3
CD3 abs. number	366	207	IgA g/l	2.93	2.33
CD4 %/ 10^9 /l	36	32	IGM g/l	1.82	2.83
CD4 abs. number	212	112			
CD8 %/ 10^9 /l	25	25			
CD8 abs. number	148	88			
CD4/CD8 1.29	1.43	1.29			

B abs number	214	98
NK cells abs number	37	25

CD3,CD4, CD8 absolute number has been decreased and more decreased after 10 day of symptom onset (Table.1 , Table.3)

PCT, CRP, D dimer and IL-6 level was increased in appliance of deterioration patient state (Table.2 ,Table. 3))

Table 2

Day after symptom onset									
PCT (ng/ml)	0.362	0.432	0.168	2,45	3.2	2.35	2.19	1.02	0.864
D dimer (mkg/ml)	0.48	0.5	0.47	3.13	19.76	3.31	3.95	2.11	1.89
CRP (mg/l)	17	39	62	99.8	121,25	62.3	30.4	29.8	16.1
IL-6 (pg/ml)	21				69.7		60		24

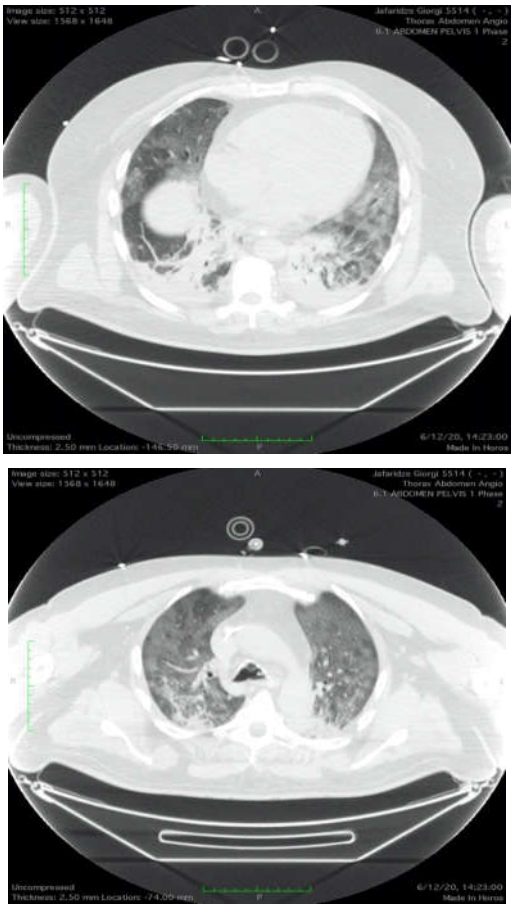

Pict.1 A Subtotal ground glass infiltrative changes are reflected on the bilateral lung parenchyma b. In which the density is higher in the lower parts, where areas of consolidation of adults and thick areas are revealed. Relatively small volume consolidations are also reflected in the upper rates. Semi-quantitative methodological analysis of computed tomography data, index of lung damage - 21 points

On the picture is presented tipical radiology sighns of covid pneumonia, subtotal ground glass infiltration, with consolidation in upper parts an interlobal pleura thickening, A small amount of secretion is released into the bilateral pleural cavity, no free air was found. With Semi-quantitative methodological analysis of computed tomography data, lung damage index was high -21 points.

Table 3

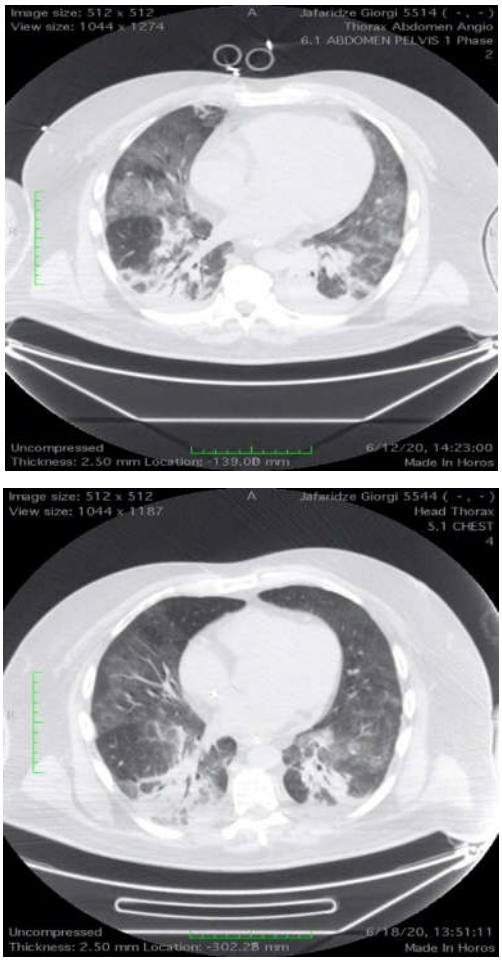

Pict 2

The intensity of subtotal ground glass infiltrative changes in the bilateral lung parenchyma is significantly reduced, although the process volume is not reduced.

Table 4

Pict 3 The severity of ground-glass infiltrative changes in the bilateral lung parenchyma is somewhat reduced, consolidation at the level of the basal segments without significant dynamics. Against the background of the compaction on the right, a single bronchiectasis is reflected.

Tabl. 5

Patient was extubated on 29 day of ilness and discharge from clinic after 48 days of admission

Case 2

Patient, women was admetted in emergency departament with fever, dry cough, dispnoea Chest computed tomography revealed bilateral pneumonia and (with Semi-quantitative methodological analysis) lung demage index --18 point. After 5 day, patient with worsened respiratory failure and dispnoea, was admetted in ICU.

Dispnoea worsened beside HFNC and NIV. CT of the chest revealed bilateral irregular infiltrates with varying density, neither emphysema, not pulmonary embolism was detected (pict .4)

Patient was intubated and started mechanical ventilation. PaO_2/FiO_2 was <200. Sputem was RT-PCR negative for SARS-COV-2. Laboratory studies showed normal leucocyte count and CRP, PCT, D dimer level. Despite the fact that RT-PCR on SARS-COV-2 was negative, we started the treatment like a respiratory distress –syndrom of covid-19.

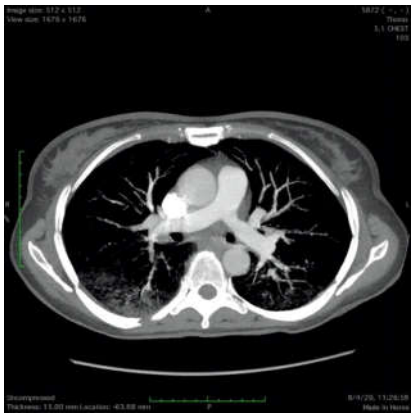

A

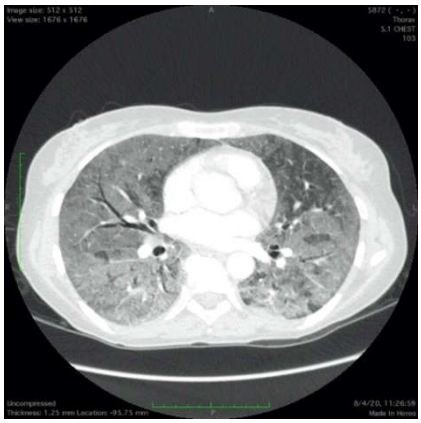

B

Pict 4 Computed tomography of the chest with contrast enhancement 08/04/2020.

Angiographic examination does not reveal a defect in filling the pulmonary trunk, bilateral main, parietal and segmental arteries, reliable signs of thrombosis. The aorta is not enlarged (pict 4 ,A)

Inflammatory changes in the phenomenon of diffuse ground glass are reflected at all levels (except for peaks) in the bilateral lung with a small basal consolidation and foci of subpleural fibrosis. Free fluid and air are not reflected in the bilateral pleural cavity (pict4,B)

D dimer, CRP and PCT level was increased gradually (Tabl.6, Tabl . 7)

D dimer	0.2	0.32	0.35	0.22	3.1	5,2	3.01	3.15	3.13	3.01
PCT	0.3	0.36	0.43	0.16	2.45	3.2	2.35	2.19	1.1	0.8
CRP	30,5	32.5			118.6	147.2	41.6	34	15.7	

Table 6

Table 7

On computed tomography of chest infiltrative changes in the diffuse ground glass phenomenon are still reflected in the bilateral lung. At the base, there are small seals and foci of subpleural fibrosis. There is little air in the right pleural space. Free fluid are not reflected in the left pleural cavity (pict.5).

Pict 5 Computed tomography of the axial section of the lung window 08/10/2020

Table 8

Patient state was aggravated. Blood analyses on Anti HBs, HBsAg, Anti HCV, was negative HSV-1 or HSV-2 IgG -- 0.5Iu/ml, herpes-zoster IgG-80g/l, toxoplasma IgG -1000g/l , Cryptococcal antigen was negative . Blood analyses on Anti - HIV antibody test was positive, CD4 abs .count- 5 , CD3 abs. count –35, CD-8 abs. count-28

The human immunodeficiency virus type 1 (HIV-1) Western blotting (immunoblotting) band patterns and the sensitivity of an HIV-1 DNA PCR assay have been determined by testing the blood of patient with AIDS.

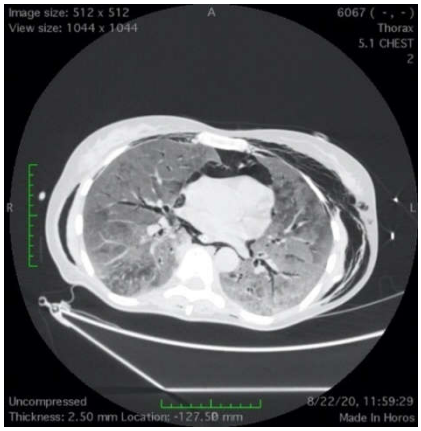

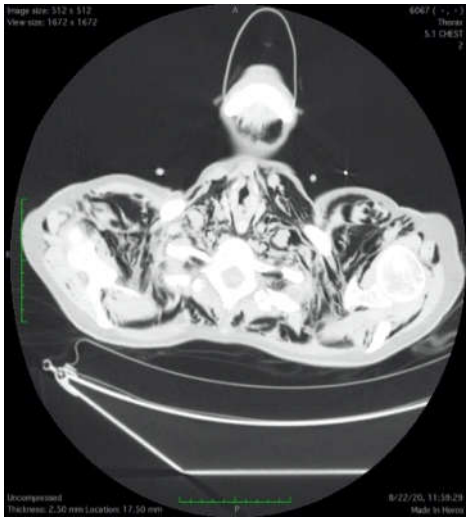

A B

Pict 6 Computed tomography of the axial section of the lung window 08/22/2020.

On computed tomography A -large amount of gas, pneumomediastinum - is found in the mediastinum at almost all levels. B. Massive emphysema of the subcutaneous soft tissue manifests itself in both the chest and neck. In the bilateral lungs at all levels, infiltrative changes such as the phenomenon of diffuse ground glass are again reflected. Free fluid and air are not reflected in the bilateral pleural cavity (pict 6.)

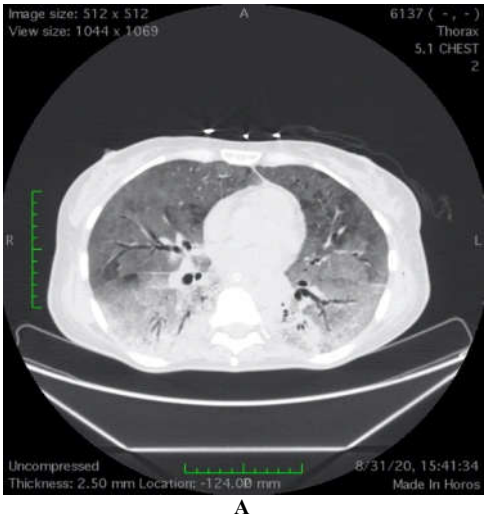

A

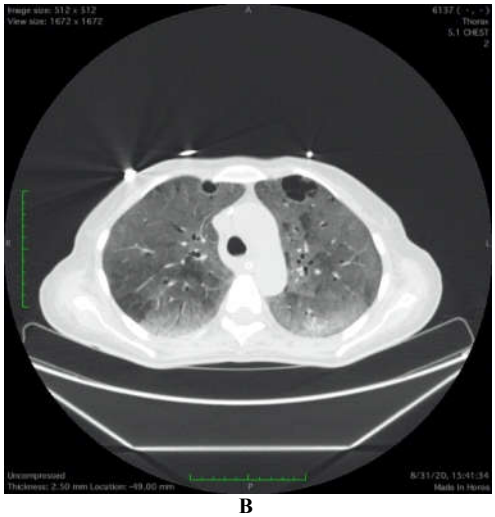

B

Pict 7 Computed tomography of the axial section of the lung window 08/31/2020.

- Air is no longer reflected on the mediastinum and soft tissues of the chest. In the bilateral lungs, infiltrative changes such as the phenomenon of diffuse ground glass are again reflected at all levels.
- In the ventral-subpleural areas of both upper extremities, cavities with air were formed, around one of them on the right fibrous-infiltrative changes are visible - a destructive process is possible. Free fluid and air are not reflected in the bilateral pleural space (pict 7).

The patient's condition, the onset of the disease and the course of the disease in both cases were similar and clinically consistent with the course of respiratory distress syndrome caused by Covid infection. The appearance of antibodies from the human immunodeficiency virus and the confirmation of this disease, pneumocyst pneumonia, made changes in the patient's treatment, improved the condition and the patient was transferred to the intensive care unit of the central infectious diseases hospital.

COVID-19 pneumonia was diverse, ranging from normal appearance to diffuse changes in the lungs. In addition, different radiological patterns was observed at different times throughout the disease course in both patient , also the time between onset of symptoms and the development of acute respiratory distress syndrome was short, ct scan obtained on day 7- 9 after symptom onset showed extensive ground glass opacities in both lungs.

CONCLUSION

Evaluation of blood tests and comparison of clinical data made it possible to diagnose a similare in the course of and CT findings, but of absolutely different disease. This comparison allow distinguish similar characteristics of different diseases and make prognostic conclusions during the course and treatment of illness.

References

1. Centers for Disease Control and Prevention. Coronavirus Disease 2019 (Covid-19): Cases and Latest Updates, 2020.
2. Pan F, Ye T, Sun P, Gui S, Liang B, Li L, Zheng D, Wang J, Hesketh RL, Yang L, Zheng C. Time Course of Lung Changes at Chest CT during Recovery from Coronavirus Disease 2019 (COVID-19) Radiology. 2020;295:715–721. [PMC free article] [PubMed] [Google Scholar]
3. Richardson S, Hirsch JS, Narasimhan M, Crawford JM, McGinn T, Davidson KW and the Northwell COVID-19 Research Consortium, Barnaby DP, Becker LB, Chelico JD, Cohen SL, Cookingham J, Coppa K, Diefenbach MA, Dominello AJ, Duer-Hefele J, Falzon L, Gitlin J, Hajizadeh N, Harvin TG, Hirschwerk DA, Kim EJ, Kozel ZM, Marrast LM, Mogavero JN, Osorio GA, Qiu M, Zanos TP. Presenting Characteristics, Comorbidities, and Outcomes Among 5700 Patients Hospitalized With COVID-19 in the New York City Area. JAMA. 2020 [PMC free article] [PubMed] [Google Scholar]
4. Tisoncik JR, Korth MJ, Simmons CP, Farrar J, Martin TR, Katze MG. Into the eye of the cytokine storm. Microbiol Mol Biol Rev. 2012;76:16–32. [PMC free article] [PubMed] [Google Scholar]

5. Radiology: Cardiothoracic Imaging. **Ng MY,** Lee EY, Yang J, Yang F, Li X, Wang H, Lui MM-s, Lo CS-Y, Leung B, Khong P-L, Hui CK-M, Yuen K-y, Kuo MD. Imaging Profile of the COVID-19 Infection: Radiologic Findings and Literature Review. 2020; 2: e200034. [Google Scholar]
6. Zhao W, Zhong Z, Xie X, Yu Q, Liu J. Relation Between Chest CT Findings and Clinical Conditions of Coronavirus Disease (COVID-19) Pneumonia: A Multicenter Study. AJR Am J Roentgenol. 2020;214:1072–1077. [PubMed] [Google Scholar]
7. Li W, Cui H, Li K, Fang Y, Li S. Chest computed tomography in children with COVID-19 respiratory infection. Pediatr Radiol. 2020;50:796–799. [PMC free article] [PubMed] [Google Scholar]
8. Kim H. Outbreak of novel coronavirus (COVID-19): What is the role of radiologists? Eur Radiol. 2020;30:3266–3267. [PMC free article] [PubMed] [Google Scholar]
9. Dennie C, Hague C, Lim RS, Manos D, Memauri BF, Nguyen ET, Taylor J. Canadian Society of Thoracic Radiology/Canadian Association of Radiologists Consensus Statement Regarding Chest Imaging in Suspected and Confirmed COVID-19. Can Assoc Radiol J. 2020:846537120924606. [PubMed] [Google Scholar]
10. Castiglioni I, Ippolito D, Interlenghi M, Monti CB, Salvatore C, Schiaffino S, Polidori A, Gandola D, Messa C, Sardanelli F. Artificial intelligence applied on chest X-ray can aid in the diagnosis of COVID-19 infection: a first experience from Lombardy, Italy. [Preprint]. In press 2020. [Google Scholar]
11. Abbas A, Abdelsamea M, Gaber M. Classification of COVID-19 in chest X-ray images using DeTraC deep convolutional neural network. [Preprint]. In press 2020. [Google Scholar]
12. Detection of human immunodeficiency virus type 1 (HIV-1) antibody by western blotting and HIV-1 DNA by PCR in patients with AIDS. J B Jackson, J S Parsons, L S Nichols, N Knoble, S Kennedy, and E M Piwowar, *J Clin Microbio*l. 1997 May; 35(5): 1118–1121.
13. Song F, Shi N, Shan F, Zhang Z, Shen J, Lu H, et al. Emerging 2019 Novel Coronavirus (2019-nCoV) Pneumonia. [published online ahead of print, 2020 Feb 6]. Radiology. 2020:200274. doi: 10.1148/radiol.2020200274 https://doi.org/10.1148/radiol.2020200274 [Links]
14. COVID-19 pneumonia: Diagnostic and prognostic role of CT based on a retrospective analysis of 214 consecutive patients from Paris, France Enora Guillo a , Ines Bedmar Gomez a , Severine Dangeard a , Souhail Bennani a , Ines Saab a,b , Mickael Tordjman a , Lea Jilet c , Guillaume Chassagnon a,b , Marie-Pierre Rev, European Journal of Radiology Clinical presentation and diagnosis of Pneumocystis pulmonary infection in patients with HIV Paul E Sax, MD, UP TO DATE
15. Recent Advances in the Diagnosis and Management of Pneumocystis Pneumonia, Sadatomo Tasaka, M.D. Tuberc Respir Dis (Seoul). 2020 Apr; 83(2): 132–140. Published online 2020 Mar 10. doi: 10.4046/trd.2020.0015
16. Reid AB, Chen SC, Worth LJ. Pneumocystis jirovecii *pneumonia* in non-HIV-infected patients: new risks and diagnostic tools. Curr Opin Infect Dis. 2011;24:534–544. [PubMed] [Google Scholar]
17. Onishi A, Sugiyama D, Kogata Y, Saegusa J, Sugimoto T, Kawano S, et al. Diagnostic accuracy of serum 1,3-beta-D-glucan for pneumocystis jiroveci pneumonia, invasive candidiasis, and invasive aspergillosis: systematic review and meta-analysis. J Clin Microbiol. 2012;50:7–15. [PMC free article] [PubMed] [Google Scholar]

How to cite this article:

Guliko Kiliptari *et al* (2021) 'The Similar Characteristics of Various Illness', *International Journal of Current Advanced Research,* 10(02), pp. 23741-23745. DOI: http://dx.doi.org/10.24327/ijcar.2021. 23745.4707

****